Available online at www.sciencedirect.com
SCIENCE DIRECT®
Journal of Nuclear Materials 329–333 (2004) 467–471
journal of nuclear materials
www.elsevier.com/locate/jnucmat

Dislocation channel formation process in V–Cr–Ti alloys irradiated below 300 °C

M. Sugiyama *, K. Fukumoto, H. Matsui

IMR/Tohoku Univ., 2-1-1 Katahira, Aoba-ku, Sendai 980-8577, Japan

Abstract

Atomic force microscopy was applied to study the slip band evolution of neutron-irradiated V–Cr–Ti alloys deformed in a tensile test. Quantitative data were obtained on the changes of the surface topography of dislocation channels and on the kinetics of dislocation channel growth up to the ultimate tensile stress. As stress approached the ultimate tensile strength, the slip bands nucleated and propagated across the specimens. As the stress increased, the interval spacing between slip bands decreased and became constant. On the other hand, the slip step height continued to increase, and indicated that the growth of individual dislocation channels occurred continuously. The conjugated and multi-slip bands in a grain were seldom observed. The evolution of dislocation channels may induce the significant loss of ductility after the UTS in V–Cr–Ti alloys.

1. Introduction

Vanadium-base alloys are attractive candidates low activation structural materials for future fusion reactors. The alloys containing 4–5% Cr and 4–5% Ti exhibit good radiation damage resistance at temperatures higher than 430 °C [1]. However, significant radiation hardening and embrittlement occur in V–4Cr–4Ti irradiated by neutrons for 100–400 °C below a few displacement per atom (dpa) [2,3]. This is one of the key issues of R&D on vanadium alloys to define the lower temperature limit for design windows of advanced fusion reactors. From the previous work [4,5], irradiation embrittlement of vanadium alloys by low temperature irradiation is caused by irradiation hardening due to the formation of dense concentrations of defect clusters during neutron irradiation. The fracture surfaces of irradiated specimens during tensile tests exhibited no intergranular surfaces but dimpled surfaces on the fracture area. A lot of tiny steps of slip band were also observed on the lateral side of fractured specimens. It is suggested that significant irradiation hardening and loss of ductility in V–4Cr–4Ti alloys is caused by the plasticity instability due to hardening produced by radiation-produced defect clusters. It is well known that for irradiation hardening, the loss of ductility is caused by formation of dislocation channeling in fcc and bcc metals irradiated at low temperatures [6,7]. The observation of dislocation channeling in V–4Cr–4Ti alloys has been reported in previous work [4]. However, the formation and propagation process of dislocation channels in irradiated V–4Cr–4Ti alloys during deformation tests is unclear. In this study atomic force microscopy (AFM) has been applied to study the evolution of dislocation channels in neutron-irradiated V–4Cr–4Ti alloys. By comparing AFM work and microstructural analysis by TEM observation, the evolution of deformation process by dislocation channeling can be discussed.

2. Experimental procedure

Two vanadium alloys of V–4Cr–4Ti–0.1Si and V–4Cr–4Ti were made by arc melting. Chemical

* Corresponding author. Tel.: +81-22 215 2067; fax: +81-22 215 2066.
E-mail addresses: sugiyama@imr.tohoku.ac.jp, fukumoto @imr.edu (M. Sugiyama).

0022-3115/$ - see front matter © 2004 Elsevier B.V. All rights reserved.
doi:10.1016/j.jnucmat.2004.04.295

composition of the alloys is listed in Table 1 in Ref. [8]. The SSJ tensile specimens ($1.6\times0.4\times0.2$ mm) were punched and annealed at 1100 °C for 2 h after a degassing treatment at 600 °C for 0.5 h in vacuum of $\sim1\times10^{-4}$ Pa. Specimens were irradiated at 307 ± 19 °C to 6.0 dpa in HFIR-11J [9]. Since the amounts of helium and hydrogen generation during irradiation were <1 ppm, the effects of helium or hydrogen are negligible. Specimens were electro-polished in order to investigate the detailed fracture surfaces and side surfaces after tensile testing. The tensile tests were conducted at room temperature and a 6.67×10^{-5}/s of strain rate (0.02 mm/min). The tensile test was periodically interrupted at applied stresses corresponding approximately to every 10–20 MPa increase of applied stress above the yield point, with the specimen removed from the testing machine for observations. Thus a systematic way of studying the surface roughness in selected grains was possible. A series of tensile tests with AFM observation or confocal laser microscope (CLM) observation were finished when the applied stress approached the ultimate tensile strength on a strain–stress curve.

The surface roughness was investigated by the use of the AFM, SPA-400, Seiko Instruments Inc. The contact imaging mode in air was used to obtain constant-force topographic images. A V-shaped silicon cantilever with a standard pyramidal tip having the radius of curvature smaller than 50 nm was applied. The optical microscope equipped with a CCD camera was used to find the appropriate spot inside circular marks on the specimen surface.

As well as AFM, the surface roughness was investigated by the use of CLM, HD-100D, Lasertec Co. Ltd. In particular, the CLM observation was more suitable to get information of surface roughness at low magnification than AFM. However the resolution of altitude on surface roughness from the CLM is inferior to AFM in order to measure the step height of slip bands.

After the specimen reached the UTS, a necking area of the deformed specimen was cut out and fabricated into a TEM specimen by electro-polishing. TEM observation was done at room temperature.

3. Results

Specimens exhibited significant irradiation hardening, close to 900 Mpa, and the total elongation was less than 0.5%. Details of the tensile properties of the irradiated specimens were described in Ref. [9].

From the CLM observations, the deformation process proceeded as follows:

(1) At a stress of 850 MPa, no changes were yet observed on the surfaces.
(2) The initial slip bands were formed at the end of the gage section of specimens when the flow stress reached to 900 MPa.
(3) The deformation band traversed the specimen width at about 45° to the tensile axis and the thicknesses of the initial deformation bands were thin.
(4) The deformation band traversed the entire specimens at stress level close to the UTS and the center of the deformation band became thinner than non-deformed parts.

The localized bands were visible on the surface by CLM and conjugated bands intersecting the original bands in a grain were rare.

The series of AFM micrographs in Fig. 1 show the evolution of surface roughness on a 0.1×0.1 mm square section on a V–4Cr–4Ti–0.1Si alloy irradiated at 300 °C. As well as AFM images, the stress–strain curve and the characteristic sequence profile of surface roughness in the cross section on AFM micrographs are shown in Fig. 1. The step height reached to 0.5 μm at 940 Mpa, close to UTS. Since the step height in deformed unirradiated specimens was a few tens nm by AFM, the slip band of neutron-irradiated V–Cr–Ti alloys was much larger than the usual slip bands for unirradiated material.

From analysis of the surface roughness profiles, it was found that the height of steps depends on stress levels. Fig. 2 show histograms of the step heights of slip band. Fig. 2(A) shows a height histogram for all slip bands. As the stress level increased, the peak step height distribution increased. Another analysis was done of distinguish the newly formed slip bands from the original slip bands as shown in Fig. 2(B). The newly formed slip bands at high stress level showed larger step heights than ones formed at lower stress levels. This suggests that the growth of slip bands depends on the stress level. Fig. 3 shows the growth of individual slip bands formed at 910 MPa in several grains. The growth rate of slip bands varied widely, however the step height did not become constant even at a stress level close to the UTS. The correlation between interval spacing and step height was also measured for individual slip bands. The averaged interval spacing and the averaged step height were plotted as a function of stress level. At low stress where the initial deformation bands occurred, the step height was still small and interval spacing remained wide. As the stress level increased, the average interval spacing became smaller and constant. On the other hand, the step height increased continuously. This suggests that the nucleation of slip bands occurred preferentially and ceased when the interval spacing between them was reached to a critical spacing. In addition, the growth of slip bands continued at higher stress levels and the slip bands newly formed at higher stress showed larger step heights. TEM micrographs of irradiated specimens de-

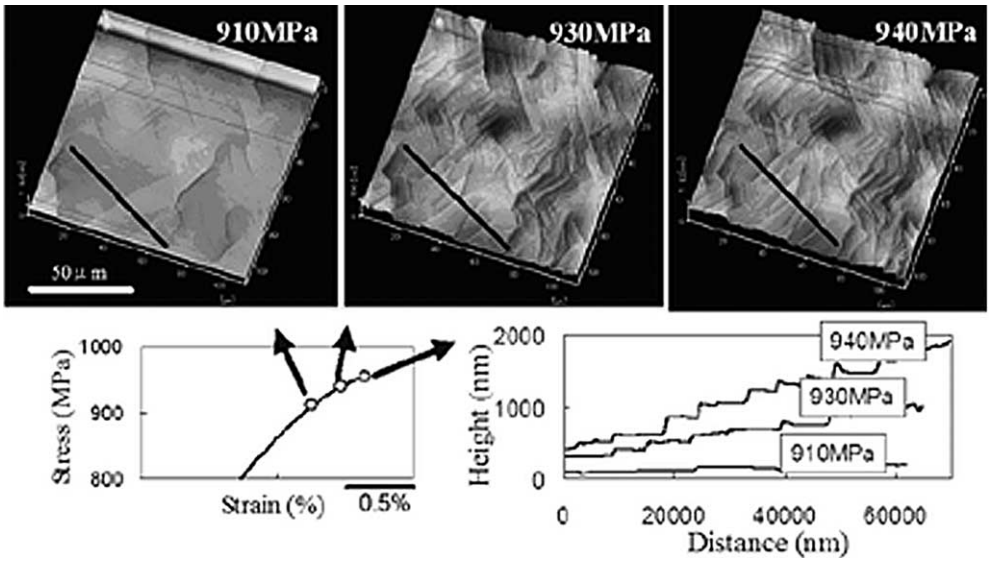

Fig. 1. AFM micrographs of the surface roughness of V–4Cr–4Ti–0.1Si with strain rate of 6.67×10^{-5}/s for different stress level. The scale of all micrographs is identical. Bottom left: The stress–strain curve indicates the stress level of each AFM images. Bottom right: the characteristic sequence profile of surface roughness in the cross section on AFM micrographs. Black lines on AMF images mark the position the trace of the height measurements.

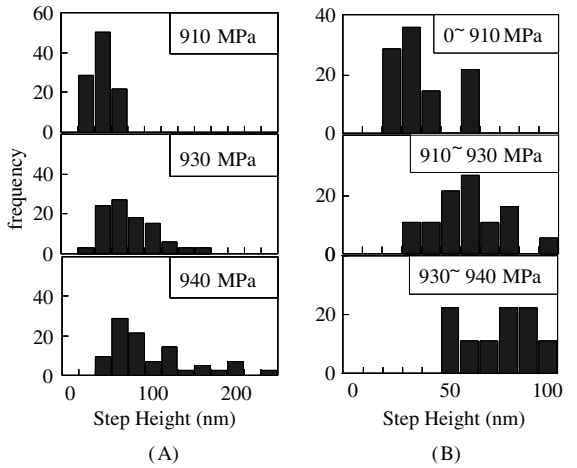

Fig. 2. Histograms of step heights for slip bands formed for different stress levels. (A) for all visible slip bands for each stress level, (B) for newly formed slip bands while a tensile test proceeded to next level.

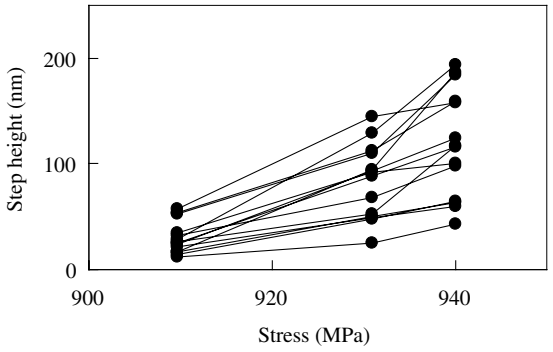

Fig. 3. The individual evolution of step heights as a function of stress level.

formed to the UTS stress are shown in Fig. 5. Outside of the deformation band, a lot of defect clusters are found, whereas inside the band no defect clusters or dislocation lines are seen. No dislocation walls or network can be observed on the interface between the matrix and the deformation band. The deformation bands entirely traversed grains and extended into the next grain across the grain boundaries. The slip planes of extended deformation bands appear to extend in the same direction as the slip plane of the original deformation bands. A step of the deformation band at a grain boundary in Fig. 5 has a height of 100 nm and is in good agreement with the results of the averaged step height at UTS as shown Fig. 4.

4. Discussion

It is clear that the deformation bands observed in TEM correspond to the steps on the surface observed in AFM, because the step heights where a deformation

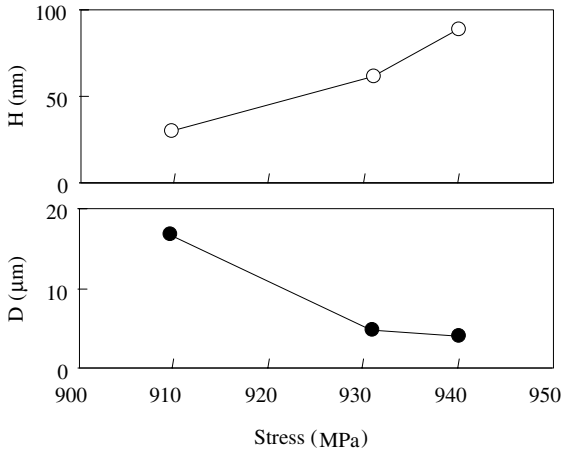

Fig. 4. Stress dependences of the averaged step height (H) and the averaged interval spacing between steps (D).

band and a grain boundary intersect and the averaged step height for the surface roughness were almost the same. Therefore the results of slip bands surface roughness obtained by AFM indicate the evolution of dislocation channels formed during tensile tests.

Formation of sip bands on the necking part showing nucleation of dislocation channels occurred at a stress above 800 MPa. Dislocation movement is impeded by a high concentration of tiny defect clusters. From a previous analysis, the estimated increase of yield stress produced by the radiation-induced defect clusters was 470 MPa for V–4Cr–4Ti irradiated at 300 °C and 5 dpa [5]. The moving dislocations swept out defect clusters as they propagate, at an applied stress that allows them to overcome the barrier of the defect clusters. Above a threshold stress for yielding, it appears that there is a stress dependence for the nucleation and propagation of dislocation channels. The increase of applied stress increases the density of dislocation channels, but the density saturated at certain stress level. This deformation process is caused by the interaction of dislocations between dislocation channels. When the interval spacing between dislocation channels is wide, up to a few tens of microns, the interaction between dislocation channels is weak and it is possible to nucleate a new dislocation channel with certain interval spacing. As the density of dislocation channels increases and interval spacing between dislocation channels is reduced to about 5 μm, the interaction between dislocation channels becomes effective and prevents new dislocation channels from nucleating. Once the density of dislocation channels saturates, the deformation process proceeds by the increase of step height in the existing dislocation channels. This model of the continuous growth of dislocation channels is different from the previous idea of propagation mechanism of dislocation channels. In the conventional model [7,10], the step growth of dislocation channels ceases at certain step heights and the conjugated slip systems begins to work in order to propagate the deformation band. In the case of Zircaloy-2 [11], conjugated slip and secondary slip of dislocation channels occurred at UTS and elongation after an abrupt drop in load appeared, indicating the onset of plastic instability. However, in the case of V–Cr–Ti alloys, the elongation after UTS and sharp load drop was very small. It is believed that the lack of conjugated and secondary slip in V–Cr–Ti alloys restricts the continuing deformation to the localized deformed areas. Intersection of dislocation channels and secondary slip of dislocation channels in a grain were not seen in TEM observation in this study. The significant loss of ductility in V–Cr–Ti alloys produced by low temperature irradiation may be caused by the evolution of dislocation channels, and the growth mechanism of the dislocation channels, in particular. It is believed that the appearance of secondary slip of dislocation channels may affects the onset of plastic instability after UTS. In the TEM work, no dislocation lines were observed inside or outside of the dislocation channels. The tangled dislocation at the interface of dislocation channels controls the activity of dislocation channels and the importance

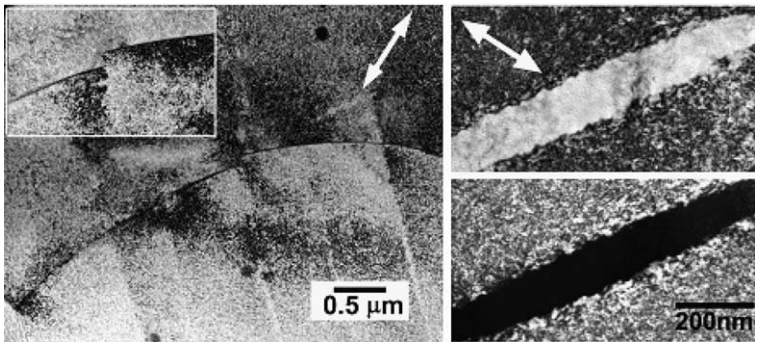

Fig. 5. TEM micrographs of a deformed V–4Cr–4Ti alloy at the UTS. The left micrograph shows dislocation channels crossing grain boundary. The right one shows the BF and DF images inside of a dislocation channel.

of dislocation structures for deformation process by dislocation channels has been reported [12]. Further study using in situ TEM observation during tensile tests is focused on the search for evidence of dislocation movement during dislocation channeling and the mechanism of removing the obstacles such as defect clusters in V–Cr–Ti.

References

[1] H. Matsui et al., J. Nucl. Mater. 233–237 (1996) 92.
[2] K. Fukumoto, H. Matsui, et al., J. Nucl. Mater. 283–287 (2000) 535.
[3] S.J. Zinkle, H. Matsui, et al., J. Nucl. Mater. 258–263 (1998) 205.
[4] P.M. Rice, S.J. Zinkle, J. Nucl. Mater. 258–263 (1998) 1414.
[5] K. Fukumoto, H. Matsui, et al., J. Nucl. Mater. 283–287 (2000) 492.
[6] Y. Huang, R.J. Arsenault, Radiat. Eff. 17 (1973) 3.
[7] J.V. Sharp, Acta Metal. 22 (1974) 449.
[8] K. Fukumoto, T. Morimura, et al., J. Nucl. Mater. 239 (1996) 170.
[9] K. Fukumoto, Y. Yan, et al., in: S. Hanada et al. (Eds.), Proceedings of the 4th Pacific Rim International Conference on Advanced Materials and Processing, vol. 1319, 2001.
[10] S. Kitajima, K. Shinohara, kinzoku-gakkai-kaihou. JIM 15 (1976) 675 (in Japanese).
[11] T. Onchi, H. Kayano, et al., J. Nucl. Mater. 88 (1980) 226.
[12] K. Shinohara, Doctor thesis, Kyushu Univ., 1990 (in Japanese).